IEEE Access
Multidisciplinary | Rapid Review | Open Access Journal

Received 5 September 2023, accepted 28 September 2023, date of publication 5 October 2023, date of current version 11 October 2023.

Digital Object Identifier 10.1109/ACCESS.2023.3322373

RESEARCH ARTICLE

Performance Analysis of Downlink Double-IRS Systems Relying on Non-Orthogonal Multiple Access

THAI-ANH NGUYEN[1], HOANG-VIET NGUYEN[1], DINH-THUAN DO[2], (Senior Member, IEEE), AND ADÃO SILVA[3,4], (Member, IEEE)

[1]Faculty of Electronics Technology, Industrial University of Ho Chi Minh City, Ho Chi Minh City 700000, Vietnam
[2]School of Engineering, University of Mount Union, Alliance, OH 44601, USA
[3]Instituto de Telecomunicações (IT), University of Aveiro, 3810-193 Aveiro, Portugal
[4]Departamento de Eletrónica, Telecomunicações e Informática (DETI), University of Aveiro, 3810-193 Aveiro, Portugal

Corresponding author: Dinh-Thuan Do (doth@mountunion.edu)

This work was supported by Fundaçao para a Ciencia e Tecnologia (FCT)/Ministry of Science, Technology and Higher Education (MCTES) through National Funds through Applicable Co-Funded European Union (EU) Funds under Project UIDB/50008/2020-UIDP/50008/2020.

ABSTRACT The intelligent reflecting surface (IRS) has emerged as a promising solution to enhance the quality of radio transmission by allowing flexible control over the direction of reflection and phase shift of electromagnetic waves. In this study, we present a downlink wireless network considering non-orthogonal multiple access (NOMA) and two IRSs to improve performance for a group of user equipment (UE) at the cell edge, when the UEs cannot reach out direct links from the base station (BS). We start by discussing the framework to design a wireless system relying on both IRS and NOMA, and then calculate the link channel statistics between the BS, IRS, and UEs with Rayleigh fading distributions using the probability density function (PDF) and cumulative distribution function (CDF). Based on these distributions, we derive closed form expressions for the outage probability (OP) for evaluating the performance of the user pair. Additionally, we compute the bit error rate (BER), the ergodic rates (ER) of the UE as functions of the signal-to-interference-plus-noise ratio (SINR) using the Chebyshev-Gauss quadrature method, and hence the complete the overall evaluation of the system's performance can be achieved. Finally, we verify the mathematical analysis through comparing with Monte-Carlo simulations and indicate that the number of IRS meta-surfaces elements as the main limiting factor to achieve better OP, ER and BER performance.

INDEX TERMS Intelligent reflecting surface, non-orthogonal multiple access, outage probability, ergodic rate.

I. INTRODUCTION

In recent years, to foster the rapid development of applications in internet of things (IoT), next wireless IoT networks are required to support billions of devices with serious constraints on spectrum efficiency, reliability, latency, capacity, and connectivity. To meet these challenging requirements, a variety of technologies have been widely applied and studied such as multiple input multiple output (MIMO), IRS and NOMA. In particular, NOMA has been recognized as a superior multiple access (MA) technique for future wireless networks due to its promising advantages, i.e. higher spectral efficiency and better fairness [1], [2], [3]. However, the NOMA technique is limited in conventional wireless networks because the user's channel gain is random and uncontrollable [4], [5], [6], [7].

With the development of material technology such as meta-surfaces that consists of many passive reflecting elements, each of which can shift the phases of the incident electromagnetic waves. These meta-surfaces are known as key component of IRS-aided wireless systems. Through intelligent phase transition configuration, IRS can increase or decrease the aggregate channel gain of different users [8], [9]. The recent studies are expected to confirm IRS get

The associate editor coordinating the review of this manuscript and approving it for publication was Zesong Fei.

more benefits to strengthen the current NOMA systems. The authors in [10] and [11] analyzed the probability of uplink outages of IRS-aided NOMA networks. In [11], the fixed and random phase transition were considered to confirm the effects of fixed and random phase transitions on the performance of the IRS-aided NOMA systems. In [12], the authors analyzed the capabilities of a IRS-aided NOMA network with multiple users. The work in [13] optimized the passive beamforming at IRS to minimize transmission power and compared the performance between IRS-aided NOMA and RIS-aided orthogonal multiple access (OMA). In [14] and [15], the studies of IRS optimization for NOMA network are presented to robust how NOMA can incorporate with IRS and to improve performance of UEs. In [16], the authors assumed the BS-IRS-UE channels as light of sight (LoS) and optimized the NOMA systems under assistance of IRS. The IRS-aided mobile edge computing (WP-MEC) system relying on wireless power transfer was developed in [17], in which time division multiple access (TDMA) and NOMA schemes are conveyed to enhance performance of uplink offloading. In [18], the authors presented an analysis of setting up IRS parameters for mobile users in the context of IRS-aided NOMA network. In [19], the authors studied an energy-saving design of the IRS-aided NOMA network. The authors in [20] considered the impacts of the phase shift of IRS meta-surfaces elements on the system performance of IRS-aided NOMA network. In the work of [21], the authors studied the NOMA and OMA downlink and uplink of NOMA-IRS system. In [22], the authors proposed a simple design of IRS-supported NOMA for downlink transmission. Conventional space division multiple access (SDMA) is first used at the BS to generate orthogonal beams using the spatial orientations of the near user's channels. The IRS-aided NOMA is then employed to ensure that additional cell edge users can also be serviced on these rays by aligning effective channel vectors related to the cell edge user with the zero directions at predefined time. In [23], the authors considered the application of the IRS to NOMA, where a BS transmits a superimposed signal to many users under assistance of the IRS. The performance of the IRS-assisted NOMA network with imperfect successive interference cancellation (ipSIC) and perfect successive interference cancellation (pSIC) was investigated by leveraging the 1-bit encoding scheme.

A. RELATED WORK

In [24], MIMO architecture is leveraged by enabling a cooperative double IRSs and the LoS propagation channels. Regarding the performance analysis, they evaluated the capacity maximization problem, which is examined as jointly optimizing of the passive beamforming matrices of the two cooperative IRSs and the transmit covariance matrix. In [25], the double-IRS aided monitoring system was explored since the IRS is implemented to improve proactive eavesdropping by jointly affecting both the suspicious and eavesdropping channels. In order to optimize the eavesdropping capability, they jointly design the passive phase shift matrices of double IRSs by considering the double-reflection links and the cooperative two single-reflection links.

In other work, the IRS-NOMA system relying on the wireless power transfer (WPT) is studied to improve the NOMA performance and efficiency of energy harvesting [26]. By jointly optimizing BS transmit beamforming vector, power splitting (PS) ratio, successive interference cancellation (SIC) decoding order and IRS phase shift, a problem of minimizing BS transmit power is presented, while taking into account the quality-of-service (QoS) requirement and energy harvested threshold of each user. In order to improve the system capacity, the work in [27] explored a novel multi-IRS assisted downlink NOMA network. The superposed signals are transmitted from the BS to multiple mobile users via multi-IRS reflection. The sum rate maximization problem is examined by optimizing reflection coefficients. The authors in [28] presented multiple antennas IRS-aided NOMA system. Their results confirmed that the transmit power scales down linearly with the BS antenna number and quadratically with the IRS element number. In [17], an IRS-aided WP-MEC system was conceived, where each device's computational task can be divided into two parts for local computing and offloading to mobile edge computing servers, respectively. Both TDMA and NOMA schemes are considered for the uplink offloading. In [29], IRS and NOMA can boost both the spectrum and the power efficiency when IRS-NOMA system operates under the support of the multi-group detection and imperfect SIC. Specifically, a group-level SIC (GSIC) is conceived to remove the decoded groups' signals, whilst the joint design of power control and equalizers is leveraged to mitigate the aggregated interference caused by NOMA, imperfect SIC, and concurrent transmissions per group. In [30], both IRS and NOMA schemes can be deployed to empower features for promising applications of unmanned aerial vehicle (UAV). In this scenario, the IRS is mounted on an UAV to assist the transmissions from a BS. The BS utilizes the UAV as a relay to serve multiple UEs on the ground. In addition to the IRS relaying links, in this work they also incorporate direct non-LoS links between the BS and UEs. The authors derived the outage probability for this system configuration.

The main results in aforementioned works have made profound contributions to research of the next generation wireless networks using both NOMA and IRS techniques, but it is still an open problem to know how many IRS could be used with respect to improve performance of user pair. Notice that none of the works above have analyzed the network performance considering whether the double IRS in the adjacent linked cells leads to improved performance if NOMA scheme can be leveraged. The analysis of the IRS-aided NOMA network performance that calculates the influence of the IRS in adjacent cells is essential and worth investigating. With a user in a IoT network using NOMA techniques combined with IRS can be affected by multiple IRSs in adjacent cells. Without loss of generality, we consider

the problem of analyzing the IoT network model using the NOMA technique combined with the IRS considering the influence of a nearby IRS. By solving this problem, we analyze the effect of multiple IRSs in adjacent cells on users in the NOMA-IRS network. On the other hand, the above works requires too complex calculations to provide limited metrics used for performance evaluations. Therefore, we aim to fill the gap by deriving low-complex closed-form expressions of ER, OP and BER.

B. MOTIVATIONS AND OUR CONTRIBUTIONS

Although many researchers have successfully studied many models of wireless systems combining IRS and NOMA, it is still necessary to present the way to determine the main parameters affecting to double IRSs-aided NOMA system (DIRS-NOMA). In our model, it is assumed that the signals originated from a BS are reflected by two IRSs to support communication for two edge users per group without a direct connections to the BS. From the proposed model, we present mathematical expressions indicating main parameters of the system and thereby evaluate the performance of the DIRS-NOMA, which is expected to be better compare with the benchmark, i.e. DIRS using OMA. The detailed contributions of this paper can be listed as follows:

1) Different from [26], [27], and [28], we consider a practical system model consisting of a BS supported by two IRSs that connect to a set group of users (each group contains two users following NOMA scheme) at the cell edge area of a dedicated coverage of the BS without having a direct connection to the BS. The system performance is expected to be enhanced since both NOMA and IRS techiques are leveraged and a new paradigm is introduced, i.e., DIRS-NOMA. From the proposed model, we calculate the performance parameters, giving closed-form mathematical expressions of the performance parameters of the system. In addition, we study the diversity order and propose an optimization algorithm for the system.
2) We first compute the instantaneous and average SINR at the users of the considered system, then derive low complexity closed-form expressions for the OP, ER and BER to completely demonstrate the system performance.
3) Finally, we find the main parameters through simulations to verify theoretical analysis. The simulation results show that the meta-surface elements of the IRS and power allocation factors in NOMA could be efficiently adjusted to boost the system performance.

C. ORGANIZATION AND NOTATIONS

The rest of this paper is organized as follows: Section II presents the mathematical framework to describe DIRS-NOMA in the downlink with respect to enhance performance of two edge users. Section III describes channel models of the BS-IRS-UE link. Section IV presents expressions to provide performance analysis, while Section V verifies the mathematical results through simulation results and more insights are discussed. Section VI draws the main remarks and conclusion.

Notations: The key notations are used in this paper, as shown in Table 1.

TABLE 1. Main denotation.

Mathemtical Operations and Functions	
$\mathbb{P}\{\cdot\}$	Probability operator
$\mathbb{E}\{\cdot\}$	Expectation operator
$f_X(\cdot)$	PDF of the Random Variable (RV) X
$F_X(\cdot)$	CDF of RV X
$\mathcal{CN}(a,b)$	Complex normal distribution with average a and variance b

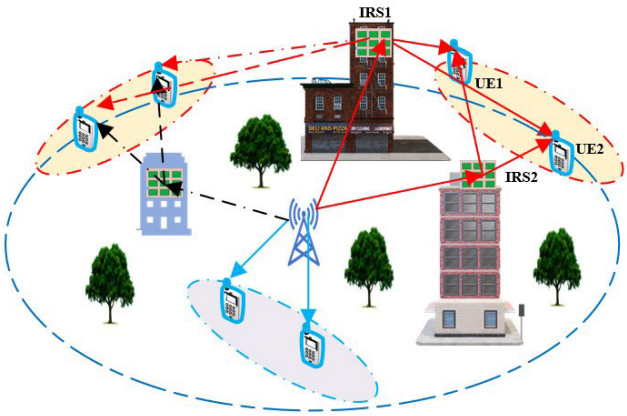

FIGURE 1. The DIRS-NOMA system model.

II. DIRS-NOMA SYSTEMS

A. SYSTEM ARCHITECTURE

We study a practical model of DIRS-NOMA network by enabling two IRSs (denoted as IRS1 and IRS2) in the downlink to achieve the better performance for many groups of users, shown in Fig. 1. In this scenario, we aim to analyze improved performance of two edge users. Under the assumption of low-cost hardware design, the BS equipped with single antenna works with two nearby IRSs to strengthen transmissions to two mobile single antenna edge users (UE1 and UE2), as shown as Fig. 1.[1] It is assumed that there is no direct signal transmissions between the BS and the UEs because of the far distance between both or existence of intermediate obstacles. The IRS has N_x reflecting elements and its reflecting matrix defined theoretically as $\Theta = diag(\beta_1 e^{j\theta_1}, \beta_2 e^{j\theta_2}, \ldots, \beta_{N_x} e^{j\theta_{N_x}})$, $j = \sqrt{-1}$, where $\beta_k \in [0,1]$ is called the amplitude of the reflectance and $\theta_k \in [0, 2\pi)$ is the phase shift angle of k-th IRS element is adjustable ($k = 1, 2, \ldots, N_x$). We denote d_{R1} as the signal transmission distance from BS to IRS1, d_{R2} is the

[1] We aim to improve the users' performance at edge area in the considered coverage related to the working BS. Therefore, it is reasonable to examine the case when the edge users can get signals through assistance of IRSs.

transmission distance from BS to IRS2, d_{11} is the distance between IRS1 and UE1, d_{12} is the distance between IRS1 and UE2, d_{21} is the distance between IRS2 and UE1, d_{22} is the distance between IRS1 and UE2.

B. BS-IRS-UE CHANNEL MODEL ANALYSIS

It is assumed a flat fading channel for all comunication links. It assume that the BS knows the channel state information (CSI). The BS-IRS and IRS-UE links can be LoS or NLoS for different practical circumstances. The channel gains between the BS and the IRSs are the same, i.e. $G_R \in C^{1\times N_x}$, and between the IRSs and the UEs are denoted by $g_u \in C^{N_x\times 1}$. They are represented as vector spaces as follows $G_R = [G_1, G_2, \ldots, G_{N_x}]$ and $g_u = [g_1, g_2, \ldots, g_{N_x}]^T$, respectively. All the elements in these channel links follow the Rayleigh fading model with a variance of 1 ($\sigma = 1$).

C. DOWNLINK SIGNAL ANALYSIS

In particular, the transmitted signal of the BS is represented as $x = \sqrt{\alpha_1 P_s} s_{UE1} + \sqrt{\alpha_2 P_s} s_{UE2}$ where P_s is the transmit power at the BS, s_{UE1} is the signal that the BS transmits to UE1, s_{UE2} is the signal that the BS transmits to UE2, α_1, α_2 represent for the power allocation factors of the BS to UE1 and UE2, respectively. It is noticed that α_1 and α_2 satisfy the condition $\alpha_1 + \alpha_2 = 1$. In the NOMA technique, the transmissions to the users are sorted based on their channel quality for the BS. According to NOMA's decoding principle, user UE1 directly decodes its own signal by treating signals intended for other users as noise. User UE2, on the other hand, sequentially decodes and discards the other user's signal, until its own signal s_{UE2} is decoded. Then the received signal at the edge users UE1 and UE2 can be represented respectively as follows:

$$y_{UE1} = \left(G_R \Theta g_u d_{R1}^{-\frac{\alpha_{G_R}}{2}} d_{11}^{-\frac{\alpha_{g_u}}{2}}\right) x + \left(G_R \Theta g_u d_{R2}^{-\frac{\alpha_{G_R}}{2}} d_{21}^{-\frac{\alpha_{g_u}}{2}}\right) x + n_{UE1}, \quad (1)$$

$$y_{UE2} = \left(G_R \Theta g_u d_{R2}^{-\frac{\alpha_{G_R}}{2}} d_{22}^{-\frac{\alpha_{g_u}}{2}}\right) x + \left(G \Theta g d_{R_1}^{-\frac{\alpha_{G_R}}{2}} d_{12}^{-\frac{\alpha_{g_u}}{2}}\right) x + n_{UE2}, \quad (2)$$

where n_{UE1} stands for the Gaussian noise at UE1, n_{UE2} is the Gaussian noise at UE2, n_{UE1} and n_{UE2} with the same variance equal to 1 ($\sigma^2_{UE1} = \sigma^2_{UE2} = \sigma^2_{UE} = 1$); α_{G_R} and α_{g_u} denote the path loss exponents of BS-IRS, and IRS-UE links, respectively.

D. SIGNAL-TO-NOISE PLUS NOISE RATIO AT USERS

The SINR is defined as the ratio of the mean effective signal power divided by the mean noise power plus the average noise power. Therefore, the SINR at the users is determined as follows.

At the UE1, the signal s_{UE2} is considered noise, then SINR is given as:

$$SINR_{UE1} = \frac{|G_R \Theta g_u|^2 r_{UE1} \alpha_1}{|G_R \Theta g_u|^2 r_{UE1} \alpha_2 + \frac{1}{\rho}}, \quad (3)$$

where $r_{UE1} = \left(d_{R1}^{-\frac{\alpha_{G_R}}{2}} d_{11}^{-\frac{\alpha_{g_u}}{2}} + d_{R2}^{-\frac{\alpha_{G_R}}{2}} d_{21}^{-\frac{\alpha_{g_u}}{2}}\right)^2$, $\rho = \frac{P_s}{\sigma^2_{UE}}$.

At the UE2, the signal s_{UE1} is considered as noise term, and then the SINR at the UE2

$$SINR_{UE2} = \frac{|G_R \Theta g_u|^2 r_{UE2} \alpha_2}{|G_R \Theta g_u|^2 r_{UE2} \alpha_1 + \frac{1}{\rho}}, \quad (4)$$

where $r_{UE2} = \left(d_{R2}^{-\frac{\alpha_{G_R}}{2}} d_{22}^{-\frac{\alpha_{g_u}}{2}} + d_{R_1}^{-\frac{\alpha_{G_R}}{2}} d_{12}^{-\frac{\alpha_{g_u}}{2}}\right)^2$.

III. BS-IRS-UE CHANNEL STATISTICS ANALYSIS

In this section, we will analyze BS-IRS-UE channel statistics.

A. PARAMETER SETTING FOR IRS

It is possible to efficiently adjust the IRS parameters to have the best BS-IRS-UE channel quality. That is, we optimize $|G_R \Theta g_u|^2 = \left|\sum_{k=1}^{N_x} \beta_k G_{Rk} g_{uk} e^{j\theta_k}\right|$, where G_{Rk} and g_{uk} are the channel gain of the k-th element of G_R and g_u respectively. This can be achieved by intelligently adjusting the θ_k phase shift for each element, meaning that the phases of all $G_{Rk} g_{uk} e^{j\theta_k}$ are set the same. After applying optimal $\{\theta_k\}$ [18], $\beta_k = \beta$, then $|G_R \Theta g_u|^2$ is given by

$$|G_R \Theta g_u|^2 = \beta^2 \left(\sum_{k=1}^{N_x} |G_{Rk}|\,|g_{uk}|\right)^2. \quad (5)$$

B. CHANNEL STATISTICS

Our performance analysis relies on the closed-form expressions CDF and PDF for RV $X = \sum_{k=1}^{N_x} |G_{Rk}|\,|g_{uk}|$, where $|G_{Rk}|$, $|g_{uk}|$ are two random variables with Rayleigh distribution. Since $|G_{Rk}|$ and $|g_{uk}|$ are two random variables with Rayleigh distribution, the product $|G_{Rk}|\,|g_{uk}|$ is also a random variable with a double Rayleigh distribution.

Theorem 1: Let X be the sum of N_x random variables with a statistically independent double Rayleigh distribution. The PDF and CDF of X can be approximated as follows [38]:

$$f_X(x) = \frac{x^m}{n^{m+1}\Gamma(m+1)} exp\left(-\frac{x}{n}\right), \quad (6)$$

$$F_X(x) = \frac{\gamma\left(m+1, \frac{x}{n}\right)}{\Gamma(m+1)}. \quad (7)$$

Proof: Please refer to Appendix A

Please note that the operators $E[\cdot]$, $Var[\cdot]$ respectively denote the statistical expectation, variance. $\Gamma(\cdot)$ is gamma function. $\gamma(\cdot)$ is incomplete Gamma function.

Figure 2 and 3 present th curves for different numbers of IRS N_x reflectors to verify the theoritical expressions

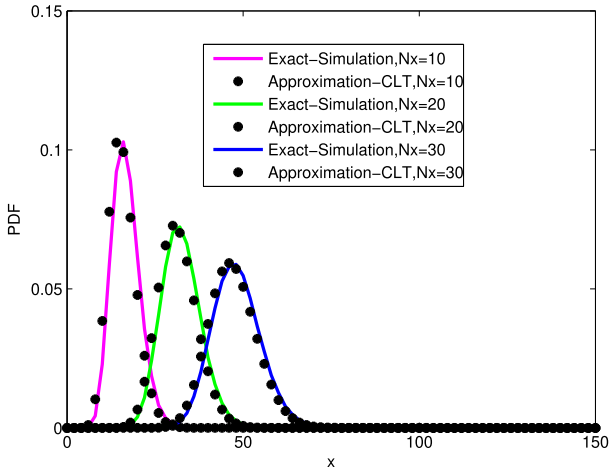

FIGURE 2. PDF of X.

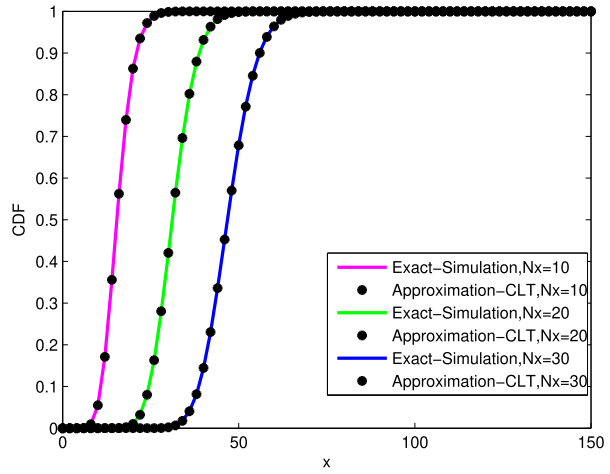

FIGURE 3. CDF of X.

IV. CALCULATION TO ACHIEVE NETWORK PERFORMANCE FOR DIRS-NOMA

In this section, we calculate the NOMA network performance parameters supported by two IRS in the downlink for the two edge users.

A. OUTAGE PROBABILITY

The OP is an important parameter commonly used to measure the performance of such DIRS-NOMA system [3]. The threshold SINR is given by $\gamma_{UE1} = 2^{\widetilde{R}_{UE1}} - 1$, $\gamma_{UE2} = 2^{\widetilde{R}_{UE2}} - 1$, where $\widetilde{R}_{UE1}$, $\widetilde{R}_{UE1}$ are target rates for UE1, UE2 respectively. In this scenario, the OPs of UE1 and UE2 are calculated as follows.

The OP for UE1 is defined by

$$OP_{UE1} = \Pr\left(SINR_{UE1} < \gamma_{UE1}\right). \tag{8}$$

In this step, (8) is rewritten as

$$OP_{UE1} = \Pr\left(\frac{|G_R\Theta g_u|^2 r_{UE1}\alpha_1}{|G_R\Theta g_u|^2 r_{UE1}\alpha_2 + \frac{1}{\rho}} < \gamma_{UE1}\right). \tag{9}$$

To make it simple, let denote $r_1 = \beta^2 r_{UE1}$, then OP_{UE1} is rewritten as:

$$OP_{UE1} = \Pr\left(\frac{X^2 r_1\alpha_1}{X^2 r_1\alpha_2 + \frac{1}{\rho}} < \gamma_{UE1}\right)$$
$$= Pr\left(X < \sqrt{\frac{\gamma_{UE1}}{r_1\left(\alpha_1 - \alpha_2\gamma_{UE1}\right)\rho}}\right). \tag{10}$$

Then, (10) can be further computed by

$$OP_{UE1} = F_X\left(\sqrt{\frac{\gamma_{UE1}}{r_1\left(\alpha_1 - \alpha_2\gamma_{UE1}\right)\rho}}\right)$$
$$= \frac{\gamma\left(m+1, \frac{1}{n}\sqrt{\frac{\gamma_{UE1}}{r_1(\alpha_1-\alpha_2\gamma_{UE1})\rho}}\right)}{\Gamma\left(m+1\right)}. \tag{11}$$

Similarly, we can achieve the OP for UE2 as follows

$$OP_{UE2} = \Pr\left(\frac{|G_R\Theta g_u|^2 r_{UE2}\alpha_1}{|G_R\Theta g_u|^2 r_{UE2}\alpha_2 + \frac{1}{\rho}} < \gamma_{UE2}\right). \tag{12}$$

By denoting $r_2 = \beta^2 r_{UE2}$, then OP_{UE2} is rewritten as

$$OP_{UE2} = \Pr\left(\frac{X^2 r_2\alpha_1}{X^2 r_2\alpha_2 + \frac{1}{\rho}} < \gamma_{UE2}\right)$$
$$= Pr\left(X < \sqrt{\frac{\gamma_{UE2}}{r_2\left(\alpha_1 - \alpha_2\gamma_{UE2}\right)\rho}}\right). \tag{13}$$

Then, (13) is rewritten by

$$OP_{UE2} = F_X\left(\sqrt{\frac{\gamma_{UE2}}{r_2\left(\alpha_1 - \alpha_2\gamma_{UE2}\right)\rho}}\right)$$
$$= \frac{\gamma\left(m+1, \frac{1}{n}\sqrt{\frac{\gamma_{UE2}}{r_1(\alpha_1-\alpha_2\gamma_{UE2})\rho}}\right)}{\Gamma\left(m+1\right)}. \tag{14}$$

B. DIVERSITY ORDER

The diversity order is a crucial performance measurement used to evaluate OP's attenuation under the impact of transmit SNR at the transmitter. In the principle, the diversity order refers to a quantity asymptotically as the SNR goes to infinity. We are interested in diversity order at finite-SNR in system design. According to [42], the diversity order is defined as

$$D_{UE}\left(\rho\right) = -\frac{\partial \log\left(OP_{UE}\right)}{\partial \log\left(\rho\right)} = -\rho\frac{\partial \log\left(OP_{UE}\right)}{\partial\rho}. \tag{15}$$

Considering for each user. the diversity order of UE1, UE2 are defined as

For UE1, by substituting (11) into (15) and putting $a_{UE1} = \frac{1}{n}\sqrt{\frac{\gamma_{UE1}}{r_1(\alpha_1-\alpha_2\gamma_{UE1})}}$, we have

$$D_{UE1}\left(\rho\right) = -\rho\frac{\partial \log\left(\gamma\left(m+1, \frac{a_{UE1}}{\sqrt{\rho}}\right)\right)}{\Gamma\left(m+1\right)\partial\rho}. \tag{16}$$

By continue to calculate (16) we have

$$D_{UE1}\left(\rho\right) = \frac{exp\left(-\frac{a_{UE1}}{\sqrt{\rho}}\right)\left(\frac{a_{UE1}}{\sqrt{\rho}}\right)^{m+1}}{\gamma\left(m+1, \frac{a_{UE1}}{\sqrt{\rho}}\right)}. \tag{17}$$

As ρ approaches infinity, the conventional diversity of UE1 can be approximated as follows

$$\bar{D}_{UE1} = \lim_{\rho\to\infty} D_{UE1}(\rho) \approx \frac{m+1}{2}. \tag{18}$$

For UE2, by substituting (14) into (15) and putting $a_{UE2} = \frac{1}{n}\sqrt{\frac{\gamma_{UE2}}{r_2(\alpha_2-\alpha_1\gamma_{UE2})}}$, we have

$$D_{UE2}(\rho) = -\rho\frac{\partial \log\left(\gamma\left(m+1, \frac{a_{UE2}}{\sqrt{\rho}}\right)\right)}{\Gamma(m+1)\,\partial\rho}. \tag{19}$$

Then, (19) can be rewritten as

$$D_{UE2}(\rho) = \frac{exp\left(-\frac{a_{UE2}}{\sqrt{\rho}}\right)\left(\frac{a_{UE2}}{\sqrt{\rho}}\right)^{m+1}}{\gamma\left(m+1, \frac{a_{UE2}}{\sqrt{\rho}}\right)}. \tag{20}$$

As ρ approaches infinity, the conventional diversity of UE2 can be approximated as follows

$$\bar{D}_{UE2} = \lim_{\rho\to\infty} D_{UE2}(\rho) \approx \frac{m+1}{2}. \tag{21}$$

The above approximation results help us to give a quantitative description of the diversity order of each user. It represents the effect of channel correlation on OP performance. The diversity order of each user with correlated channels is smaller than that of uncorrelated channels, and channel correlation will reduce OP performance.

C. ERGODIC RATE

The ER is one of the important metrics used to evaluate the performance of such DIRS-NOMA system. The ERs of the UEs in the system are defined as follows:

$$R_{UE1} = E\left(\log_2\left(1+SINR_{UE1}\right)\right), \tag{22}$$

$$R_{UE2} = E\left(\log_2\left(1+SINR_{UE2}\right)\right). \tag{23}$$

Theorem 2: Let $Y = \frac{X^2 rp}{X^2 rq+\frac{1}{\rho}}$, where r, p, q are constants and X is a RV with a double Rayleigh distribution. The CDF function of Y is defined as follows [38]:

$$F_Y(\gamma) = \frac{\gamma\left(m+1, \frac{y}{n}\right)}{\Gamma(m+1)}, \tag{24}$$

where $y = \sqrt{\frac{\tilde{\gamma}}{r(p-q\tilde{\gamma})\rho}}$.

Proof: Please refer to Appendix B.

To calculate the ER for UE1, we set $Y = \frac{X^2 r_1\alpha_1}{X^2 r_1\alpha_2+\frac{1}{\rho}}$, and its corresponding CDF function is defined as follows:

$$F_Y(\gamma_{UE1}) = \frac{\gamma\left(m+1, \frac{y_1}{n}\right)}{\Gamma(m+1)}, \tag{25}$$

where $y_1 = \sqrt{\frac{\gamma_{UE1}}{r_1(\alpha_1-\alpha_2\gamma_{UE1})\rho}}$. Then, R_{UE1} is approximated as follows:

$$R_{UE1} \approx -\int_0^{\alpha_{UE1}} \log_2(1+\gamma_{UE1})\,d\left(1-F_Y(\gamma_{UE1})\right)$$

$$= \frac{1}{\ln(2)}\int_0^{\alpha_{UE1}} \frac{1-F_Y(\gamma_{UE1})}{1+\gamma_{UE1}}\,d\gamma_{UE1}, \tag{26}$$

$$R_{UE1} = \log_2(1+\alpha_{UE1}) - \frac{1}{\ln(2)\Gamma(m+1)}$$

$$\times \int_0^{\alpha_{UE1}} \frac{\Gamma(m+1)-\gamma\left(m+1, \frac{y_1}{n}\right)}{1+\gamma_{UE1}}\,d\gamma_{UE1}, \tag{27}$$

where $\alpha_{UE1} = \frac{\alpha_1}{\alpha_2}$.

By denoting $t = \frac{2\gamma_{UE1}}{\alpha_{UE1}} - 1$, then R_{UE1} is rewritten as follows:

$$R_{UE1} = \log_2(1+\alpha_{UE1}) - \frac{\alpha_{UE1}}{2\ln(2)\Gamma(m+1)}$$

$$\times \int_{-1}^{1} \frac{\Gamma(m+1)-\gamma(m+1, t_{UE1})}{1+\frac{1}{2}\alpha_{UE1}(1+t)}\,dt, \tag{28}$$

where $t_{UE1} = \frac{1}{n}\sqrt{\frac{\frac{1}{2}\alpha_{UE1}(1+t)}{r_1\left(\alpha_1-\frac{1}{2}\alpha_2\alpha_{UE1}(1+t)\right)\rho}}$.

In the next step, by leveraging the Chebyshev-Gauss quadrture we can calculate R_{UE1} as follows:

$$R_{UE1} = \log_2(1+\alpha_{UE1}) - \frac{\alpha_{UE1}}{2\ln(2)\Gamma(m+1)}$$

$$\times \sum_{i=1}^{u_1} \varpi_1 \frac{\Gamma(m+1)-\gamma(m+1, z_1)}{1+\frac{1}{2}\alpha_{UE1}(1+t_i)}\sqrt{1-t_i^2}, \tag{29}$$

where $\varpi_1 = \frac{\pi}{u_1}$; $t_i = cos\frac{(2i-1)\pi}{2u_1}$ and $z_1 = \frac{1}{n}\sqrt{\frac{\frac{1}{2}\alpha_{UE1}(1+t_i)}{r_1\left(\alpha_1-\frac{1}{2}\alpha_2\alpha_{UE1}(1+t_i)\right)\rho}}$.

Similarly, we can compute R_{UE2} as follows:

$$R_{UE2} = \log_2(1+\alpha_{UE2}) - \frac{\alpha_{UE2}}{2\ln(2)\Gamma(m+1)}$$

$$\times \sum_{i=1}^{u_2} \varpi_2 \frac{\Gamma(m+1)-\gamma(m+1, z_2)}{1+\frac{1}{2}\alpha_{UE2}(1+t_i)}\sqrt{1-t_i^2}, \tag{30}$$

where $\alpha_{UE2} = \frac{\alpha_2}{\alpha_1}$ and $z_2 = \frac{1}{n}\sqrt{\frac{\frac{1}{2}\alpha_{UE2}(1+t_i)}{r_2\left(\alpha_1-\frac{1}{2}\alpha_2\alpha_{UE2}(1+t_i)\right)\rho}}$.

Remark 1: Considering $Y = \frac{X^2 r_1\alpha_1}{X^2 r_1\alpha_2+\frac{1}{\rho}}$, when $\rho \to +\infty$ then $\frac{1}{\rho} \to 0$ which leads to $Y = \frac{\alpha_1}{\alpha_2}$, then R_{UE1} has an upper asymptotic value $R_{UE1} \approx \log_2(1+\alpha_{UE1})$. Similarly, R_{UE2} has an upper asymptotic value $R_{UE2} \approx \log_2(1+\alpha_{UE2})$.

D. OPTIMIZATION ALGORITHM

In DIRS-NOMA downlinks, multiple data streams are stacked in the source domain, and user decoding is based on a sequential denoising mechanism. The performance of DIRS-NOMA depends heavily on the power division between the data streams and the power allocation problem involved. From the equity point of view, we investigate power allocation techniques that ensure fairness to downlink users according to instantaneous CSI at the transmitter. The calculation results show that the overall system performance can be significantly improved if DIRS-NOMA allocates energy to each user properly. We leverage the results of [41] to suggest the optimal energy allocation algorithm for DIRS-NOMA as follows. The ER of the users can be rewritten as follows:

$$R_{UE1}(\alpha) = \log_2\left(1 + \frac{|G_R\Theta g_u|^2 d_{UE1}\alpha_1 P}{|G_R\Theta g_u|^2 d_{UE1}\alpha_2 P + 1}\right), \quad (31)$$

$$R_{UE2}(\alpha) = \log_2\left(1 + \frac{|G_R\Theta g_u|^2 d_{UE2}\alpha_2 P}{|G_R\Theta g_u|^2 d_{UE2}\alpha_1 P + 1}\right), \quad (32)$$

where $d_{UE1} = \left(d_{R1}^{-\frac{\alpha_{G_R}}{2}} d_{11}^{-\frac{\alpha_{g_u}}{2}} + d_{R2}^{-\frac{\alpha_{G_R}}{2}} d_{21}^{-\frac{\alpha_{g_u}}{2}}\right)^2$ and $d_{UE2} = \left(d_{R2}^{-\frac{\alpha_{G_R}}{2}} d_{22}^{-\frac{\alpha_{g_u}}{2}} + d_{R_1}^{-\frac{\alpha_{G_R}}{2}} d_{12}^{-\frac{\alpha_{g_u}}{2}}\right)^2$. There is a continuous channel response on the transmitter side, the user's ER can be allocated according to their instantaneous channel condition. The max-min fairness used to maximize the user ER is built according to the results of [41] as follows.

$$\max_{\alpha_i i\in\{1;2\}} \min R_{UEi}(\alpha), \quad (33a)$$

$$s.t: \sum_{i=1}^{2} \alpha_i \le 1 \quad (33b)$$

$$0 \le \alpha_i \quad (33c)$$

It is noted that the problem (33) is a quasi-convex problem. Because the constraints of (33) are convex because $\sum_{i=1}^{2} \alpha_i \le 1$ and $0 \le \alpha_i$ are linear. A function is convex, all its subsets must be convex, that is, $S_t = \left\{\min_i R_{UEi}(\alpha) \ge t, i \in \{1;2\}\right\}$ is convex set for all real numbers t. However, the set S_t is concave with all real numbers t, since the constraints $R_{UEi}(\alpha) \ge t, i \in \{1;2\}$ can be expressed as the corresponding linear inequalities for UE1, UE2 as follows:

Considering on UE1, we have

$$\alpha_1 P|G_R\Theta g_u|^2 \ge \left(2^t - 1\right)\left(\alpha_2 P|G_R\Theta g_u|^2 + \sigma_{UE}^2\right). \quad (34)$$

Considering on UE2, we have

$$\alpha_2 P|G_R\Theta g_u|^2 \ge \left(2^t - 1\right)\left(\alpha_1 P|G_R\Theta g_u|^2 + \sigma_{UE}^2\right). \quad (35)$$

Let s^* be the optimal objective function value for the quasi-concave problem (33). For a particular constant value t, if a linear program find α_i subject to constraints (33b), (33c), (34) or (35) is feasible, then $s^* \ge t$, otherwise $s^* \le t$. Similarly, one can solve a linear program $\min_{\alpha} \sum_{i\in\{1;2\}} \alpha_i$ subject to constraints (33c) and (34) or (35) and check if the solution is satisfied (33b). By appropriately limiting t through a bisection procedure (Algorithm 1), the optimal solution for (33), with the desired precision ε, can be obtained by solving a series of linearities above.

Algorithm 1 Optimal Solution to Problem (33)

Initialization. $t_{Lp} = 0$, $t_{UB} = \log\left(1 + \frac{|G_R\Theta g_u|^2 P}{\sigma_{UE}^2}\right)$.

while $(t_{UB} - t_{Lb} \ge \varepsilon)$ **do**
  Set $t = \frac{t_{UB}+t_{Lb}}{2}$; Solve Lp to obtain α^{Lp}
  if $\sum_{i=1}^{2} \alpha_i^{Lp} \le 1$ **then**
    Set $t_{Lb} = t$, $\alpha^* = \alpha^{Lp}$, $s^* = t$
  else
    Set $t_{UB} = t$.
  end
end

Since the problem (33) is a quasi-convex problem, it satisfies the necessary and sufficient conditions of Karush-Kuhn-Tucker, so the optimal solution of the power allocation factor for UEs could be given respectively for UE1 and UE2 by:

Considering on UE1, we have

$$\alpha_1 = \frac{2^t - 1}{P|G_R\Theta g_u|^2}\left(\alpha_2 P|G_R\Theta g_u|^2 + \sigma_{UE}^2\right). \quad (36)$$

Considering on UE2, we have

$$\alpha_2 = \frac{2^t - 1}{P|G_R\Theta g_u|^2}\left(\alpha_1 P|G_R\Theta g_u|^2 + \sigma_{UE}^2\right). \quad (37)$$

E. AVERAGE BER

The BER is a typical measurement parameter used to evaluate the accuracy of data transmission. BER can be defined as $P_e = aE\left[Q\left(\sqrt{bSINR}\right)\right]$, where a and b depend on the type of modulation key [31]. The BER of two users can be determined as follows. The BER for UE1 can be given as

$$P_{e_{UE1}} = aE\left[Q\left(\sqrt{b\gamma_{UE1}}\right)\right] = a\int_0^\infty Q\left(\sqrt{b\gamma_{UE1}}\right) dF_Y(\gamma_{UE1}). \quad (38)$$

For different binary modulation schemes, a uniform BER expression is given by [31]

$$P_{e_{UE1}} = \frac{a^b}{2\sqrt{2\pi}\Gamma(b)} \times \int_0^{\infty} exp\left(-\frac{b\gamma_{UE1}}{2}\right)\gamma_{UE1}^{a-1}F_Y(\gamma_{UE1})\,d\gamma_{UE1}, \quad (39)$$

where $F_Y(\gamma_{UE1}) = \frac{\gamma\left(m+1,\frac{1}{n}\sqrt{\frac{\gamma_{UE1}}{r_1(\alpha_1-\alpha_2\gamma_{UE1})\rho}}\right)}{\Gamma(m+1)}$. Then, we can calculate the approximate value of $P_{e_{UE1}}$ as follows.

$$P_{e_{UE1}} \approx \frac{1}{2} - \frac{a^b}{2\sqrt{2\pi}\Gamma(b)} \times \int_0^{\alpha_{UE1}} exp\left(-\frac{b\gamma_{UE1}}{2}\right)\gamma_{UE1}^{a-1}F_Y(\gamma_{UE1})\,d\gamma_{UE1}. \quad (40)$$

Using differential phase shift key (DPSK) ($a = b = 1$), by denoting $t = \frac{2\gamma_{UE1}}{\alpha_{UE1}} - 1$ then $P_{e_{UE1}}$ is rewritten as follows:

$$P_{e_{UE1}} \approx \frac{1}{2} - \frac{\alpha_{UE1}}{4\sqrt{2\pi}\Gamma(1)} \times \int_{-1}^{1} exp\left(-\frac{\alpha_{UE1}(t+1)}{4}\right)F_Y\left(\frac{\alpha_{UE1}(t+1)}{2}\right)dt. \quad (41)$$

By applying the Chebyshev-Gauss quadrature we can calculate $P_{e_{UE1}}$ as follows:

$$P_{e_{UE1}} = \frac{1}{2} - \frac{\alpha_{UE1}}{4\sqrt{2\pi}\Gamma(1)}\sum_{i=1}^{u_1}\varpi_1 exp\left(-\frac{\alpha_{UE1}(t_i+1)}{4}\right) \times F_Y\left(\frac{\alpha_{UE1}(t_i+1)}{2}\right)\sqrt{1-t_i^2}, \quad (42)$$

where $\varpi_1 = \frac{\pi}{u_1}$; $t_i = cos\frac{(2i-1)\pi}{2u_1}$.

By doing the similar steps of computing $P_{e_{UE1}}$ we can calculate $P_{e_{UE2}}$ as follows:

$$P_{e_{UE2}} = \frac{1}{2} - \frac{\alpha_{UE2}}{4\sqrt{2\pi}\Gamma(1)}\sum_{i=1}^{u_2}\varpi_2 exp\left(-\frac{\alpha_{UE2}(t_i+1)}{4}\right) \times F_Y\left(\frac{\alpha_{UE2}(t_i+1)}{2}\right)\sqrt{1-t_i^2}, \quad (43)$$

where $\varpi_2 = \frac{\pi}{u_2}$; $t_i = cos\frac{(2i-1)\pi}{2u_2}$.

F. DIRS-OMA PERFORMANCE ANALYSIS

We can consider DIRS-OMA as a necessary benchmark to highlight the benefits of DIRS-NOMA. For a fair comparison, we assume that each UE receives its own resources as in the NOMA case.

The expression of SINR at UEs in DIRS-OMA scheme can be determined as follows:

At UE1, the signal s_{UE2} is considered noise, we have SINR at UE1 as

$$SINR_{UE1}^{OMA} = \frac{|G_R\Theta g_u|^2 r_{UE1}}{|G_R\Theta g_u|^2 r_{UE1} + \frac{1}{\rho}}. \quad (44)$$

Similarly, SINR at UE2 is given by

$$SINR_{UE2}^{OMA} = \frac{|G_R\Theta g_u|^2 r_{UE1}}{|G_R\Theta g_u|^2 r_{UE2} + \frac{1}{\rho}}. \quad (45)$$

In the next step, the OPs of UE1 and UE2 can be calculated respectively as follow

$$OP_{UE1}^{OMA} = \Pr\left(SINR_{UE1}^{OMA} < \gamma_{UE1}^{OMA}\right). \quad (46)$$

Next, OP_{UE1}^{OMA} is expressed by

$$OP_{UE1}^{OMA} = \Pr\left(\frac{X^2 r_1}{X^2 r_1 + \frac{1}{\rho}} < \gamma_{UE1}^{OMA}\right) = Pr\left(X < \sqrt{\frac{\gamma_{UE1}^{OMA}}{r_1\left(1-\gamma_{UE1}^{OMA}\right)\rho}}\right). \quad (47)$$

It is noted that (47) can be computed as

$$OP_{UE1}^{OMA} = F_X\left(\sqrt{\frac{\gamma_{UE1}^{OMA}}{r_1\left(1-\gamma_{UE1}^{OMA}\right)\rho}}\right) = \frac{\gamma\left(m+1,\frac{1}{n}\sqrt{\frac{\gamma_{UE1}^{OMA}}{r_1(1-\gamma_{UE1}^{OMA})\rho}}\right)}{\Gamma(m+1)}. \quad (48)$$

Similarly, the OP performance of UE2 is presented as

$$OP_{UE2}^{OMA} = \Pr\left(\frac{X^2 r_2}{X^2 r_2 + \frac{1}{\rho}} < \gamma_{UE2}^{OMA}\right) = Pr\left(X < \sqrt{\frac{\gamma_{UE2}^{OMA}}{r_2\left(1-\gamma_{UE2}^{OMA}\right)\rho}}\right). \quad (49)$$

Then, (49) can be rewritten as

$$OP_{UE2}^{OMA} = F_X\left(\sqrt{\frac{\gamma_{UE2}^{OMA}}{r_2\left(1-\gamma_{UE2}^{OMA}\right)\rho}}\right) = \frac{\gamma\left(m+1,\frac{1}{n}\sqrt{\frac{\gamma_{UE2}^{OMA}}{r_2(1-\gamma_{UE2}^{OMA})\rho}}\right)}{\Gamma(m+1)}, \quad (50)$$

where $\gamma_{UE1}^{OMA} = 2^{2\widetilde{R}_{UE1}} - 1$, $\gamma_{UE2}^{OMA} = 2^{2\widetilde{R}_{UE2}} - 1$.

Remark 2: Since the expressions of (11) and (14) are expected to explore main impacts on the system performance, we fortunately find that the performance of two users in DIRS-NOMA mostly depend on ρ. It means that the transmit SNR at the BS contributes to the improvement of performance at user end. The configuration of IRS also plays an important role to adjust performance metrics, such as OP, ER, and BER.

TABLE 2. Simulation parameter setting.

Parameters	Notation	Values
Power splitting factors	$\{\alpha_1, \alpha_2\}$	$\{0.1, 0.9\}$
Power splitting factors	$\{\alpha_1, \alpha_2\}$	$\{0.7, 0.3\}$
Bandwidth [18]	B	$1Mhz$
Complex reflection coefficient [18]	β	0.9
Distance between BS and IRS_1 [18]	d_{R_1}	40m
Distance between BS and IRS_2 [18]	d_{R_2}	40m
Distance between IRS_1 and UE_1 [18]	d_{11}	10m
Distance between IRS_1 and UE_2 [18]	d_{12}	30m
Distance between IRS_2 and UE_2 [18]	d_{22}	10m
Distance between IRS_2 and UE_1 [18]	d_{21}	30m
Path-loss exponents [18]	$\alpha_G, \alpha_{g_1}, \alpha_{g_2}$	2.5
Target data-rates [18]	$\widetilde{R}_{UE1}, \widetilde{R}_{UE2}$	0.1Mbps
Number of points CG-GL [18]	u_1, u_2	100

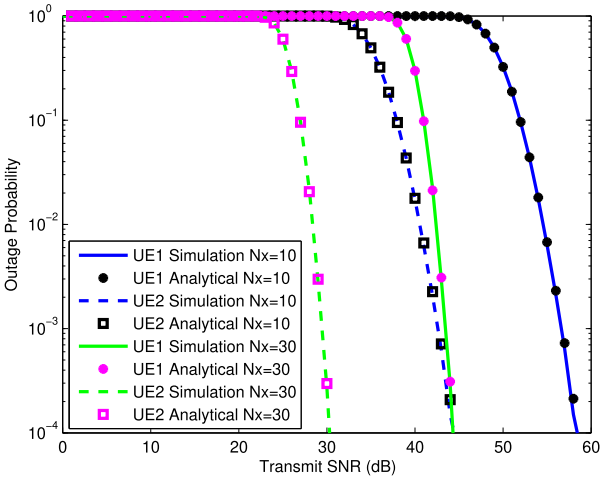

FIGURE 4. The OPs of UEs, $\alpha_1 = 0.1$, $\alpha_2 = 0.9$.

Remark 3: To compare the performance of DIRS-NOMA and DIRS-OMA, we try to find what are the main parameters affecting the improvement of DIRS-NOMA system. Interestingly, the power allocation factors α_1, α_2 in DIRS-NOMA make the main impact to the differences between DIRS-NOMA and DIRS-OMA.

To confirm what are main factors affecting the system performance, we simulate to verify expressions presented in the previous sections. The simulation results are shown in section V.

V. SIMULATION RESULTS AND DISCUSSION

In this section, we simulate the DIRS-NOMA system to verify the derived expressions using the Monte Carlo simulation method. The simulation settings are shown in Table 2.

In Figure 4, we verify the expressions in (11) and (14) to look at users' performance versus the transmit SNR at the BS. Scpecifically, we consider some configurations of the IRSs, which have 10 and 30 meta-surface elements, power allocation factors $\alpha_1 = 0, 1$ (for UE1) and $\alpha_2 = 0, 9$ (for UE2). The results of the OPs of UEs show that

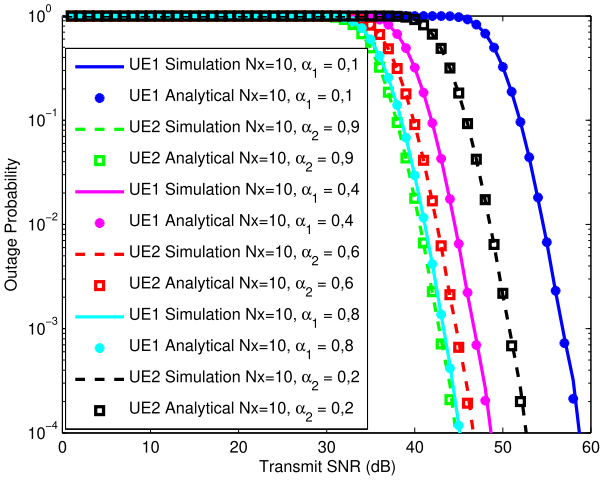

FIGURE 5. The OPs of UEs with varying power allocation factors.

all simulation and analysis curves are identical. When the number of meta-surface elements of the IRS is changed, the performance gap of OP curves can be observed clearly. In addition, it is further confirmed that the power allocation factors also affect to the OP characteristics of the users. To this end, we simulated the OPs of the UEs by changing values of α_1, α_2, shown in Figure 5.

In Figure 5, we simulate OPs of two users when the transmit SNR changes from 0 to 50. The other parameter settings are, 10 and 30 meta-surface elements, power allocation factors $\alpha_1 = 0, 1$, $\alpha_1 = 0, 4$, $\alpha_1 = 0, 8$ for UE1 and $\alpha_2 = 0, 9$, $\alpha_2 = 0, 6$, $\alpha_2 = 0, 2$ for UE2, respectively. The good matching curves between Monte-Carlo simulations and mathematical analysis results confirm that our derived expressions are correct. From the analysis results in Figures 4 and 5, OPs depend on not only on the number of IRS meta-surface elements but also the power allocation factors. Specifically, the larger the number of meta-surface elements of the IRS, the better OP can be achieved. The larger the power allocation factor gap is assigned among two users, the larger gap between two curves of OPs of the two users. Thus, if we design the DIRS-NOMA with reasonable number of meta-surface elements and power allocation factors, the system performance can be improved significantly.

In Figure 6, we simulate how the ERs of UEs when the transmit SNR at the BS comes from 10 to 60. We also consider two cases of the IRS, i.e. 10 and 30 meta-surface elements, power allocation factors $\alpha_1 = 0.1$ for UE1 and $\alpha_1 = 0.9$ for UE2. The curves of the ER using mathematical analysis are consistent with the simulation results, which confirms the exactness of our derived expressions for ER performance. When the number of IRS meta-surface elements is large, the slope of the ER characteristics is large, and a higher ER level can be reached. In addition, we see that the power allocation also affects the ER characteristics of the two users. Similarly, Figure 7 demonstrates how power allocation factors give influences on ERs.

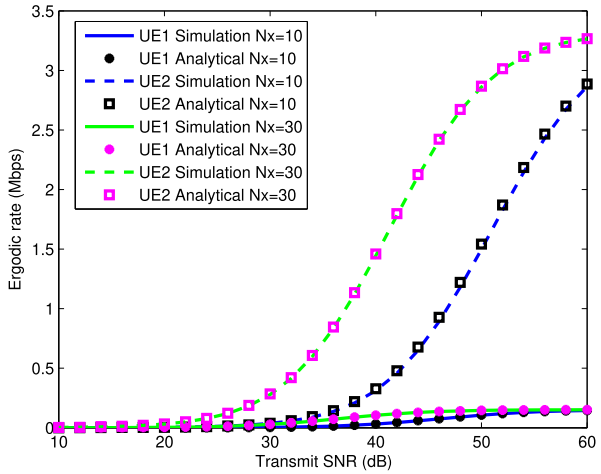

FIGURE 6. ERs of UEs, $\alpha_1 = 0.1$, $\alpha_2 = 0.9$.

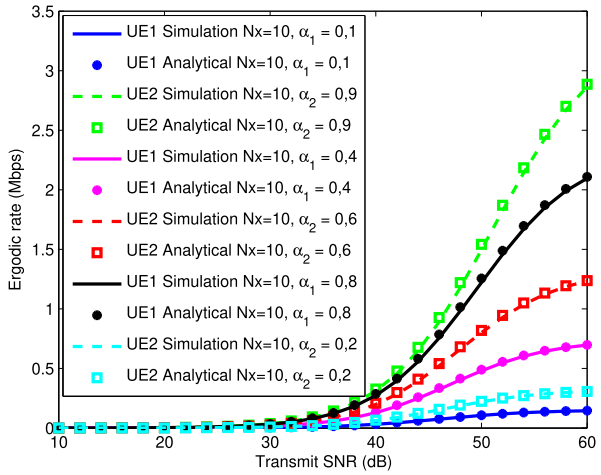

FIGURE 7. ERs of UEs obtained with varying power allocation factors.

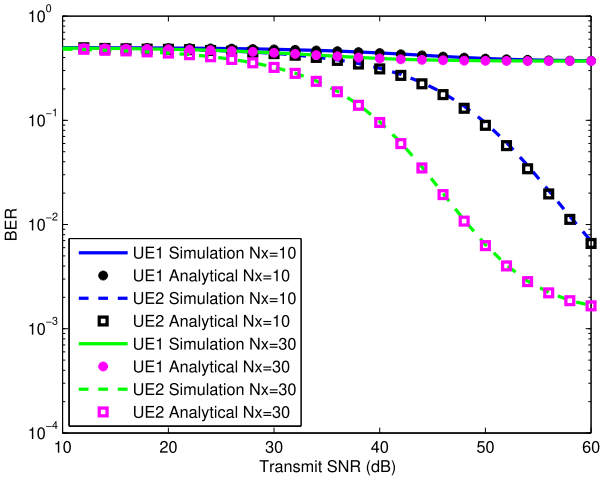

FIGURE 8. BERs of UEs obtained when $\alpha_1 = 0.1$, $\alpha_2 = 0.9$.

In Figure 8, we simulate the BER of user pair with the given settings of IRS and power allocation factors. We find that the higher the SINR, the more disparity between the

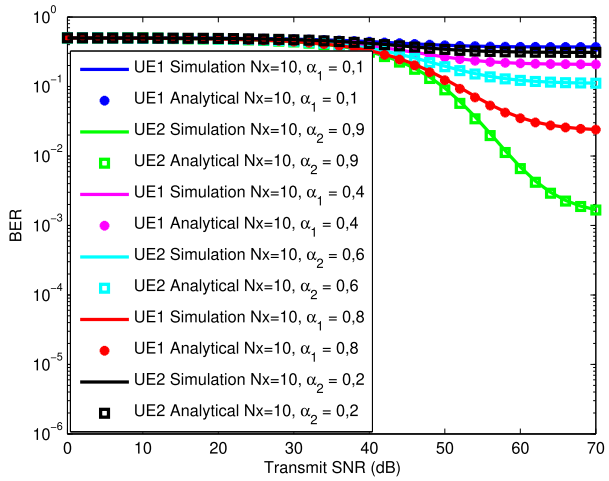

FIGURE 9. BERs of UEs obtained with varying power allocation factors.

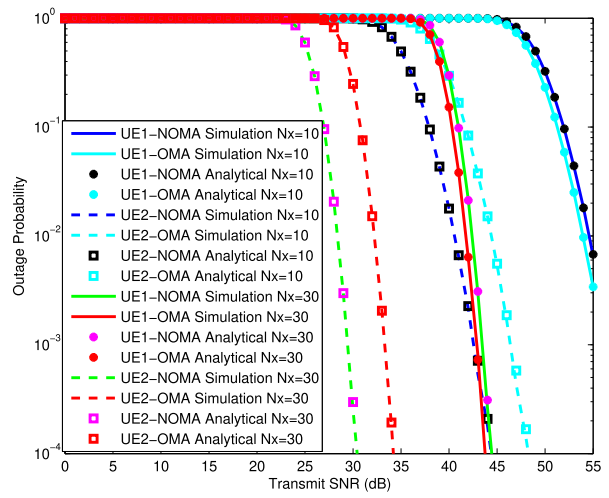

FIGURE 10. OPs of UEs obtained when $\alpha_1 = 0.1$, $\alpha_2 = 0.9$ for both DIRS-NOMA and DIRS-OMA systems.

analysis and simulation results. On the other hand, BER also depends on the number of meta-surface elements of the IRS. In particular, as the number of IRS elements increases, the slope of the graph increases. In addition, it can be clearly seen in Figure 9 the power allocation factors also affect the BER characteristics of the user pair significantly.

Next, we show performance both DIRS-NOMA and DIRS-OMA systems in Figure 10. For UE1: In case the IRS has 10 meta-surface, the transmit power ranges from 10 to 20, the OP characteristics of DIRS-NOMA and DIRS-OMA are the same since they have the same slope. The gap among two OP curves can be seen clearer at high SNR regime, i.e. SNR is greater than 50. In the case of IRS with 30 meta-surface, the similar observations can be obtained. The performance of UE2 can be analyzed similar as UE1.

VI. CONCLUSION

In this paper, we have presented the performance analysis of a DIRS-NOMA system for two edge users. Through

the analysis and insights discussions, NOMA technology gives flexible power allocation factors assigned to users while the IRS can adjust phase of signals to significantly improve the system's performance. To evaluate the system performance, we assumed that the power allocation is fixed in lots of simulation, which affects the levels of differences among performance of the two user pair in terms of the OP, the ER as well as the BER performance metrics. Further, optimization of such power allocation is provided in simple computation. The impact of transmit SNR on the trends of the system performance is considered through diversity order. In addition, we confirmed that the number of meta-surface elements of the IRS and the power allocation factors can be crucial to achieve expected system performance. Further, our framework demonstrates the superiority of the double IRS and NOMA schemes which is considered as guidelines to design future IoT systems.

APPENDIX A
PROOF OF PROPOSITION 1

We denote X as the sum of N_x random variables with statistically independent double Rayleigh distribution, according to [22, ch.2.2.2]. The PDF of X can be approximated as the first term of the Laguerre series expansion defined as follows:

$$f_X(x) = \frac{x^m}{n^{m+1}\Gamma(m+1)} exp\left(-\frac{x}{n}\right), \tag{51}$$

where $m = \frac{\Omega_1^2}{\Omega_2} - 1$, $n = \frac{\Omega_2}{\Omega_1}$, with $\Omega_1 = E[X]$ and $\Omega_2 = 4Var[X]$. Since $|G_{Rk}|$ and $|g_{uk}|$ are two random variables with a Rayleigh distribution that have a variance of 1 and are statistically independent, $\Omega_1 = N_x\frac{\pi}{2}$ and $\Omega_2 = 4N_x\left(1-\frac{\pi^2}{16}\right)$. From the PDF function we can calculate the CDF as follows:

$$F_X(x) = \int_0^x f_X(t)dt = \frac{1}{n^{m+1}\Gamma(m+1)}\Im(x), \tag{52}$$

where $\Im(x) = \int_0^x t^m exp\left(\frac{-t}{n}\right)dt$, set $z = \frac{t}{n}$, by considering [23, eq(8.350/1)] we have the interesting formula of $\Im(x)$ as $\Im(x) = n^{m+1}\gamma\left(m+1, \frac{x}{n}\right)$. By replacing $\Im(x)$ in (7), we have the CDF as follows:

$$F_X(x) = \frac{\gamma\left(m+1, \frac{x}{n}\right)}{\Gamma(m+1)}. \tag{53}$$

The proof of Proposition 1 is completed.

APPENDIX B
PROOF OF PROPOSITION 2

We have:

$$F_Y(y) = Pr(Y < \tilde{\gamma}). \tag{54}$$

Substituting $Y = \frac{X^2rp}{X^2rq+\frac{1}{\rho}}$ in (40) we get (41)

$$F_Y(y) = Pr\left(\frac{X^2rp}{X^2rq+\frac{1}{\rho}} < \tilde{\gamma}\right). \tag{55}$$

We can rewrite (41) as follows

$$F_Y(y) = Pr\left(X^2rp < \tilde{\gamma}\left(X^2rq+\frac{1}{\rho}\right)\right). \tag{56}$$

Then, $F_Y(y)$ is given by

$$F_Y(y) = Pr\left(X^2r(p-q\tilde{\gamma}) < \frac{\tilde{\gamma}}{\rho}\right). \tag{57}$$

In this step, we compute $F_Y(y)$ as

$$F_Y(y) = Pr\left(X < \sqrt{\frac{\tilde{\gamma}}{r(p-q\tilde{\gamma})\rho}}\right). \tag{58}$$

Also, deriving the CDF of Y as

$$F_Y(y) = \frac{\gamma\left(m+1, \frac{y}{n}\right)}{\Gamma(m+1)}. \tag{59}$$

The proof of Proposition 2 is completed.

REFERENCES

[1] J. Tang, J. Luo, M. Liu, D. K. C. So, E. Alsusa, G. Chen, K.-K. Wong, and J. A. Chambers, "Energy efficiency optimization for NOMA with SWIPT," *IEEE J. Sel. Topics Signal Process.*, vol. 13, no. 3, pp. 452–466, Jun. 2019.
[2] D.-T. Do, A.-T. Le, Y. Liu, and A. Jamalipour, "User grouping and energy harvesting in UAV-NOMA system with AF/DF relaying," *IEEE Trans. Veh. Technol.*, vol. 70, no. 11, pp. 11855–11868, Nov. 2021.
[3] M.-S. Van Nguyen, D.-T. Do, S. Al-Rubaye, S. Mumtaz, A. Al-Dulaimi, and O. A. Dobre, "Exploiting impacts of antenna selection and energy harvesting for massive network connectivity," *IEEE Trans. Commun.*, vol. 69, no. 11, pp. 7587–7602, Nov. 2021.
[4] Z. Chen, Z. Ding, X. Dai, and G. K. Karagiannidis, "On the application of quasi-degradation to MISO-NOMA downlink," *IEEE Trans. Signal Process.*, vol. 64, no. 23, pp. 6174–6189, Dec. 2016.
[5] D.-T. Do, T.-L. Nguyen, K. M. Rabie, X. Li, and B. M. Lee, "Throughput analysis of multipair two-way replaying networks with NOMA and imperfect CSI," *IEEE Access*, vol. 8, pp. 128942–128953, 2020.
[6] D.-T. Do, T. T. Nguyen, C.-B. Le, M. Voznak, Z. Kaleem, and K. M. Rabie, "UAV relaying enabled NOMA network with hybrid duplexing and multiple antennas," *IEEE Access*, vol. 8, pp. 186993–187007, 2020.
[7] D.-T. Do, A.-T. Le, and B. M. Lee, "NOMA in cooperative underlay cognitive radio networks under imperfect SIC," *IEEE Access*, vol. 8, pp. 86180–86195, 2020.
[8] M.-S.-V. Nguyen, D.-T. Do, A. Vahid, S. Muhaidat, and D. Sicker, "Enhancing NOMA backscatter IoT communications with RIS," *IEEE Internet Things J.*, early access, Aug. 25, 2023, doi: 10.1109/JIOT.2023.3308786.
[9] A. Sikri, A. Mathur, G. Verma, and G. Kaddoum, "Distributed RIS-based dual-hop mixed FSO-RF systems with RIS-aided jammer," in *Proc. IEEE 94th Veh. Technol. Conf. (VTC-Fall)*, Norman, OK, USA, Sep. 2021, pp. 1–5.
[10] B. Tahir, S. Schwarz, and M. Rupp, "Analysis of uplink IRS-assisted NOMA under Nakagami-*m* fading via moments matching," *IEEE Wireless Commun. Lett.*, vol. 10, no. 3, pp. 624–628, Mar. 2021.
[11] Z. Ding, R. Schober, and H. V. Poor, "On the impact of phase shifting designs on IRS-NOMA," *IEEE Wireless Commun. Lett.*, vol. 9, no. 10, pp. 1596–1600, Oct. 2020.

[12] X. Mu, Y. Liu, L. Guo, J. Lin, and N. Al-Dhahir, "Capacity and optimal resource allocation for IRS-assisted multi-user communication systems," *IEEE Trans. Commun.*, vol. 69, no. 6, pp. 3771–3786, Jun. 2021.

[13] B. Zheng, Q. Wu, and R. Zhang, "Intelligent reflecting surface-assisted multiple access with user pairing: NOMA or OMA?" *IEEE Commun. Lett.*, vol. 24, no. 4, pp. 753–757, Apr. 2020.

[14] J. Zhu, Y. Huang, J. Wang, K. Navaie, and Z. Ding, "Power efficient IRS-assisted NOMA," *IEEE Trans. Commun.*, vol. 69, no. 2, pp. 900–913, Feb. 2021, doi: 10.1109/TCOMM.2020.3029617.

[15] M. Fu, Y. Zhou, and Y. Shi, "Intelligent reflecting surface for downlink non-orthogonal multiple access networks," in *Proc. IEEE Globecom Workshops (GC Wkshps)*, Waikoloa, HI, USA, Dec. 2019, pp. 1–6.

[16] G. Yang, X. Xu, and Y.-C. Liang, "Intelligent reflecting surface assisted non-orthogonal multiple access," in *Proc. IEEE Wireless Commun. Netw. Conf. (WCNC)*, Seoul, South Korea, May 2020, pp. 1–6.

[17] G. Chen, Q. Wu, W. Chen, D. W. K. Ng, and L. Hanzo, "IRS-aided wireless powered MEC systems: TDMA or NOMA for computation offloading?" *IEEE Trans. Wireless Commun.*, vol. 22, no. 2, pp. 1201–1218, Feb. 2023.

[18] T. Hou, Y. Liu, Z. Song, X. Sun, Y. Chen, and L. Hanzo, "Reconfigurable intelligent surface aided NOMA networks," *IEEE J. Sel. Areas Commun.*, vol. 38, no. 11, pp. 2575–2588, Nov. 2020.

[19] F. Fang, Y. Xu, Q.-V. Pham, and Z. Ding, "Energy-efficient design of IRS-NOMA networks," *IEEE Trans. Veh. Technol.*, vol. 69, no. 11, pp. 14088–14092, Nov. 2020.

[20] D.-T. Do, A.-T. Le, N.-D.-X. Ha, and N.-N. Dao, "Physical layer security for Internet of Things via reconfigurable intelligent surface," *Future Gener. Comput. Syst.*, vol. 126, pp. 330–339, Jan. 2022.

[21] Y. Cheng, K. H. Li, Y. Liu, K. C. Teh, and H. V. Poor, "Downlink and uplink intelligent reflecting surface aided networks: NOMA and OMA," *IEEE Trans. Wireless Commun.*, vol. 20, no. 6, pp. 3988–4000, Jun. 2021.

[22] Z. Ding and H. V. Poor, "A simple design of IRS-NOMA transmission," *IEEE Commun. Lett.*, vol. 24, no. 5, pp. 1119–1123, May 2020.

[23] X. Yue and Y. Liu, "Performance analysis of intelligent reflecting surface assisted NOMA networks," *IEEE Trans. Wireless Commun.*, vol. 21, no. 4, pp. 2623–2636, Apr. 2022.

[24] Y. Han, S. Zhang, L. Duan, and R. Zhang, "Double-IRS aided MIMO communication under LoS channels: Capacity maximization and scaling," *IEEE Trans. Commun.*, vol. 70, no. 4, pp. 2820–2837, Apr. 2022.

[25] Y. Cao, L. Duan, M. Jin, and N. Zhao, "Cooperative double-IRS aided proactive eavesdropping," *IEEE Trans. Commun.*, vol. 70, no. 9, pp. 6228–6240, Sep. 2022.

[26] Z. Li, W. Chen, Q. Wu, K. Wang, and J. Li, "Joint beamforming design and power splitting optimization in IRS-assisted SWIPT NOMA networks," *IEEE Trans. Wireless Commun.*, vol. 21, no. 3, pp. 2019–2033, Mar. 2022.

[27] L. Wang, T. Zhou, and T. Xu, "Sum rate maximization for multi-IRS assisted downlink NOMA with mobile users," in *Proc. IEEE Int. Conf. Commun. (ICC)*, Seoul, South Korea, May 2022, pp. 3778–3783.

[28] Z. Sun and Y. Jing, "On the performance of multi-antenna IRS-assisted NOMA networks with continuous and discrete IRS phase shifting," *IEEE Trans. Wireless Commun.*, vol. 21, no. 5, pp. 3012–3023, May 2022.

[29] H. Wang, Z. Shi, Y. Fu, and S. Fu, "On intelligent reflecting surface-assisted NOMA uplinks with imperfect SIC," *IEEE Wireless Commun. Lett.*, vol. 11, no. 7, pp. 1518–1522, Jul. 2022.

[30] S. Solanki, J. Park, and I. Lee, "On the performance of IRS-aided UAV networks with NOMA," *IEEE Trans. Veh. Technol.*, vol. 71, no. 8, pp. 9038–9043, Aug. 2022.

[31] S. Primak, V. Kontorovich, and V. Lyandres, *Stochastic Methods and Their Applications to Communications: Stochastic Differential Equations Approach*. West Sussex, U.K.: Wiley, 2004.

[32] I. S. Gradshteyn and I. M. Ryzhik, *Table of Integrals, Series, and Products*, 6th ed. New York, NY, USA: Academic, 2000.

[33] I. S. Ansari, S. Al-Ahmadi, F. Yilmaz, M.-S. Alouini, and H. Yanikomeroglu, "A new formula for the BER of binary modulations with dual-branch selection over generalized-K composite fading channels," *IEEE Trans. Commun.*, vol. 59, no. 10, pp. 2654–2658, Oct. 2011.

[34] A. Lozano, A. M. Tulino, and S. Verdu, "High-SNR power offset in multiantenna communication," *IEEE Trans. Inf. Theory*, vol. 51, no. 12, pp. 4134–4151, Dec. 2005.

[35] I. S. Gradshteyn and I. M. Ryzhik, *Table of Integrals, Series, and Products*, 7th ed. Amsterdam, The Netherlands: Elsevier, 2007.

[36] Y. Liu, Z. Qin, M. Elkashlan, A. Nallanathan, and J. A. McCann, "Non-orthogonal multiple access in large-scale heterogeneous networks," *IEEE J. Sel. Areas Commun.*, vol. 35, no. 12, pp. 2667–2680, Dec. 2017.

[37] Z. Wei, L. Yang, D. W. K. Ng, J. Yuan, and L. Hanzo, "On the performance gain of NOMA over OMA in uplink communication systems," *IEEE Trans. Commun.*, vol. 68, no. 1, pp. 536–568, Jan. 2020.

[38] C. Zhong and Z. Zhang, "Non-orthogonal multiple access with cooperative full-duplex relaying," *IEEE Commun. Lett.*, vol. 20, no. 12, pp. 2478–2481, Dec. 2016.

[39] N. Bhargav, C. R. N. D. Silva, Y. J. Chun, É. J. Leonardo, S. L. Cotton, and M. D. Yacoub, "On the product of two κ–μ random variables and its application to double and composite fading channels," *IEEE Trans. Wireless Commun.*, vol. 17, no. 4, pp. 2457–2470, Apr. 2018.

[40] A. A. Boulogeorgos and A. Alexiou, "Performance analysis of reconfigurable intelligent surface-assisted wireless systems and comparison with relaying," *IEEE Access*, vol. 8, pp. 94463–94483, 2020.

[41] S. Timotheou and I. Krikidis, "Fairness for non-orthogonal multiple access in 5G systems," *IEEE Signal Process. Lett.*, vol. 22, no. 10, pp. 1647–1651, Oct. 2015.

[42] T. Wang, M.-A. Badiu, G. Chen, and J. P. Coon, "Outage probability analysis of STAR-RIS assisted NOMA network with correlated channels," *IEEE Commun. Lett.*, vol. 26, no. 8, pp. 1774–1778, Aug. 2022.

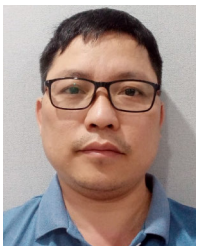

THAI-ANH NGUYEN was born in Vietnam. He received the degree in electrical and electronic engineering from the Vietnam Military Technical Academy, in 2009, and the master's degree from the Ho Chi Minh University of Technology and Education, Vietnam, in 2018, with a major in electronics and telecommunications. Currently, he is pursuing the Ph.D. degree with the Industrial University of Ho Chi Minh City, Vietnam. Dr. Hoang-Viet Nguyen and Dr. Dinh-Thuan Do are his instructors. From 2009 to 2023, he was a Lecturer with the Naval Technical College, Vietnam. His research interest includes the application of intelligent reflective surfaces in telecommunications networks.

HOANG-VIET NGUYEN was born in Ho Chi Minh City, Vietnam, in 1978. He received the master's degree in optical communications from Osaka Prefecture University, Osaka, Japan, in June 2004, and the Ph.D. degree in optical communications from Hunan University, Changsha, China, in 2015. Since 2007, he has been a Lecturer with the Industrial University of Ho Chi Minh City, Ho Chi Minh City. His current research interests include high-speed optical communication, wavelength division multiplexing, radio over fiber, cognitive radio, and satellite communication.

DINH-THUAN DO (Senior Member, IEEE) received the M.Sc. and Ph.D. degrees in electrical engineering from Vietnam National University Ho Chi Minh City (VNU-HCM), in 2007 and 2012, respectively. Prior to joining academia, he was a Senior Engineer in the telecommunications industry with VinaPhone Mobile Network (the biggest cellular network provider in Vietnam) (2003–2009). Before to joining the University of Mount Union, he was a Research Scientist with the University of Colorado Denver, in 2022, and The University of Texas at Austin, in 2021, and an Assistant Professor with Asia University, Taiwan, from 2020 to 2021. He is currently serving as an Associate Editor for IEEE TRANSACTION ON VEHICULAR TECHNOLOGY and *Computer Communications* (Elsevier). He has also served as a Lead Guest Editor/Guest Editor in more than 20 special issues of journals, such as *Physical Communications* (Elsevier) and *Annals of Telecommunications* (Elsevier). His publications include over 120 SCIE/SCI-indexed journal articles, five edited books (IET, Springer), and over 50 international conference papers. He was a recipient of the 2015 Golden Globe Award by Vietnamese Ministry of Science and Technology (top ten outstanding scientists nationwide). He also received Medal of Creative Young Talents, in 2015. He was named in top 14 highly cited scientists at Asia University, in 2021 (Stanford's list of top 2% scientists in the world, in October 2020, October 2021, and October 2022). He was rewarded as the Best Editor of *ICT Express* (Elsevier's journal), in 2023.

ADÃO SILVA (Member, IEEE) received the M.Sc. and Ph.D. degrees in electronics and telecommunications from the University of Aveiro, in 2002 and 2007, respectively. He is currently an Associate Professor with Departamento de Eletrónica, Telecomunicações e Informática (DETI), University of Aveiro, and a Senior Researcher with Instituto de Telecomunicaes. He has participated in several national and European projects. He has led several research projects in broadband wireless communications at the national level. He served as a member of the TPC at several international conferences. He is also an Associate Editor of IEEE ACCESS and *IET Signal Processing*. His research interests include multicarrier-based systems, cooperative networks, precoding, multiuser detection, and massive MIMO and millimeter wave communications. Within these research topics, he has published more than 150 technical papers in international journals and conference proceedings.